

## Surface Layering at the Mercury-Electrolyte Interface

A. Elsen,<sup>1</sup> B. M. Murphy,<sup>1,\*</sup> B. M. Ocko,<sup>2</sup> L. Tamam,<sup>3</sup> M. Deutsch,<sup>3</sup> I. Kuzmenko,<sup>4</sup> and O. M. Magnussen<sup>1</sup>

<sup>1</sup>*Institute for Experimental and Applied Physics, Christian-Albrechts-University Kiel, 24098 Kiel, Germany*

<sup>2</sup>*Condensed Matter Physics & Materials Sciences Department, Brookhaven National Laboratory, New York 11973, USA*

<sup>3</sup>*Physics Department and The Institute of Nanotechnology and Advanced Materials, Bar-Ilan University, Ramat-Gan 52900, Israel*

<sup>4</sup>*CMC-CAT, Advanced Photon Source, Argonne National Laboratory, Argonne, Illinois 60439, USA*

(Received 24 September 2009; published 12 March 2010)

X-ray reflectometry reveals atomic layering at a liquid-liquid interface—mercury in a 0.01 M NaF solution. The interface width exceeds capillary wave theory predictions and displays an anomalous dependence on the voltage applied across it, displaying a minimum positive of the potential of zero charge. The latter is explained by electrocapillary effects and an additional intrinsic broadening of the interface profile, tentatively assigned to polarization of the conduction electrons due to the electric field of the electrochemical double layer at the interface.

DOI: 10.1103/PhysRevLett.104.105501

PACS numbers: 61.05.cm, 61.25.Mv, 68.05.Cf

Liquid-liquid interfaces play an important role in many areas of soft condensed matter, chemistry, and biology, e.g., in wet synthesis, emulsions, and biomembranes. However, their structure, dynamics, and properties on the nanometer scale are still largely unknown, mainly due to the experimental challenges in studying these deeply buried interfaces. In particular, no data exist on the atomic-scale local structure at these interfaces. Hence, it is difficult to assess the validity of structural inferences drawn for liquid-liquid interfaces from the related, more accessible, liquid-gas or liquid-solid ones.

A particularly extensively studied liquid-liquid system is the interface between mercury and electrolyte solutions. This model system for an electrified interface represents the earliest example of an electric potential induced variation of an interface property, namely, the interfacial tension  $\gamma$ , through an effect known as electrocapillarity [1]. Hg electrodes have been instrumental in key experiments verifying traditional [2–4] and modern [5] theories of the electrochemical double layer and have been extensively used in studies of electrochemical adsorption, charge transfer, and chemical analytics. In spite of this importance, atomic-resolution data on the structure of the Hg-electrolyte interface is currently inaccessible.

Unlike dielectric liquids, liquid metals were predicted to show a unique atomic layering at their liquid-vapor interface, induced by the sharp decrease in the conduction electrons' density upon transition from the conducting liquid to the insulating vapor [6]. This prediction was confirmed when x-ray reflectivity (XR) measurements of the surfaces of Hg [7,8] and of other liquid metals and alloys [9–13] revealed distinct quasi-Bragg peaks originating in this layering, at a momentum transfer position  $q_z \approx 2\pi/\sqrt{3}r$ , corresponding to the atomic radius  $r$  of each metal. For Hg,  $q_z = 2.2 \text{ \AA}^{-1}$  [7] and  $r = 1.60 \text{ \AA}$ . Later studies of the Hg-vapor interface showed this spacing to be independent of temperature  $T$ , but revealed a pronounced

increase in surface roughness with increasing  $T$  [8]. While the latter is expected from the increasing amplitude  $\sigma_T$  of the capillary waves present at every liquid surface, the Hg-vapor interface is the only one among the tens studied to date that exhibits an increase beyond the  $\sigma_T \sim \sqrt{T/\gamma}$  dependence predicted by capillary wave (CW) theory [8].

In electrochemical environments  $\gamma$ , and hence  $\sigma_T$ , depend on the electric potential  $\phi$  of the Hg metal electrode, with  $\gamma(\phi)$  being maximal at the potential of zero charge (PZC) where the electrode carries no excess charge [14]. Furthermore, the strong electric field of the electrochemical double layer may influence the ionic or electronic distribution at the liquid-liquid interface [15] and specifically the surface layering. The only previous XR study of a Hg-electrolyte interface, did not consider  $\phi$  dependence, and extended to  $q_z \leq 0.8 \text{ \AA}^{-1}$  only, far too small to achieve atomic resolution [16]. The detailed potential-dependent XR study presented here provides, for the first time, clear experimental evidence that the atomic Hg layering exists also at an electrochemical liquid-liquid interface, and reveals how the presence of the electrolyte and  $\phi$  influence the interfacial structure.

Measurements were carried out at the liquid surface diffractometer, beam line ID-9, Advanced Photon Source, at an x-ray wavelength  $\lambda = 0.5605 \text{ \AA}$ . A Kel-F cell with a 4 cm diameter Hg trough and glass windows was employed [Fig. 1(c)]. Using a potentiostat (Compactstat, Ivium Technologies) and a Pt wire counterelectrode the potential was controlled versus a Hg/Hg<sub>2</sub>SO<sub>4</sub> electrode (Schott), connected to the cell via a liquid bridge. All potentials  $\phi$  are quoted relative to the PZC. The 0.01 M NaF electrolyte comprised of 99.995% pure NaF (Sigma Aldrich) and Milli-Q water. Cyclic voltammetry and differential capacitance impedance spectroscopy measurements were compared with Grahame's [17] results and confirmed the absence of electrochemically active surface contaminations over periods of up to 4 days.

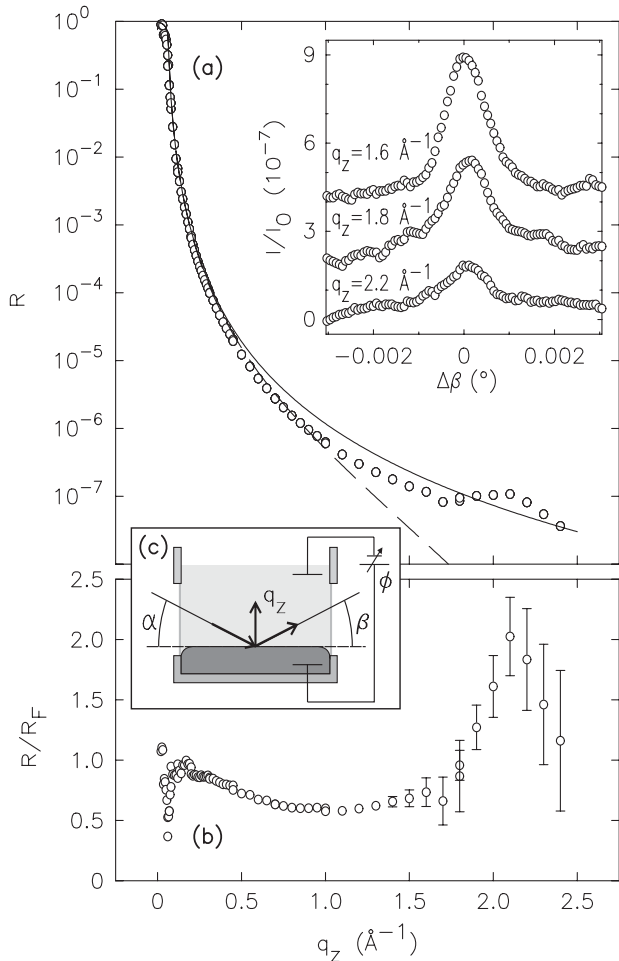


FIG. 1. (a) Measured ( $\circ$ ) and calculated (lines) XR curves for the Hg/0.01 M NaF electrolyte interface at  $\phi = 0.28$  V. Solid line: Fresnel reflectivity  $R_F(q_z)$  of an ideal interface. Dashed line:  $R_F$  modified by  $1.3 \text{ \AA}$  roughness and the Hg atomic form factor. Inset: Beam profiles at the listed  $q_z$ 's measured at  $\phi = 0.05$  V, (b) Fresnel normalized  $R(q_z)$  of (a). (c) XR measurement geometry.

XR measures the intensity fraction  $R(q_z)$  reflected from the interface at incidence and reflection angles  $\alpha$  and  $\beta = \alpha$ , respectively, where  $q_z = (4\pi/\lambda) \sin \alpha$  [Fig. 1(c)]. The height of the incidence slit was adjusted to optimize the illuminated sample area. The vertical and horizontal detector acceptances were set to  $0.4^\circ$  and  $0.08^\circ$ . The background, due to scattering by the Hg and electrolyte bulks, was measured by offsetting the detector by  $0.08^\circ$  out of the plane of reflection, and subtracted from the specular signal.

The measured  $R(q_z)$  for  $\phi = 0.28$  V is shown in Fig. 1(a). The quasi-Bragg peak at  $\sim 2.15 \text{ \AA}^{-1}$  provides clear evidence for interfacial Hg layering. The beam profiles [Fig. 1(a), inset], measured by scanning  $\beta$  across the specular position  $\beta = \alpha$ , exhibit a pronounced specular signal above background even at  $q_z > 1.5 \text{ \AA}^{-1}$ , where  $R \leq 10^{-7}$ . For comparison, calculated XR curves for an ideal

interface  $R_F$  (solid line), and for a  $1.3 \text{ \AA}$  wide monotonic interface (dashed line) are also shown in Fig. 1(a).

The quasi-Bragg peak is more pronounced in the  $R/R_F$  plot [Fig. 1(b)].  $R/R_F$  decreases monotonically for  $0 < q_z < 1 \text{ \AA}^{-1}$ , in agreement with the limited  $q_z$  range results of Bosio *et al.* [16], and then increases up to the quasi-Bragg peak position. The close similarity between this  $R(q_z)$  curve and that of the Hg-vapor interface [7], and the good agreement in the peak positions, indicate a very similar atomic layering at both interfaces.

A selection of  $R/R_F$  curves measured at other  $\phi$  values is shown in Fig. 2(a). A clear variation of the layering peak's intensity with  $\phi$ , peaking at  $R/R_F \approx 2$  at  $\phi \approx 0.3$  V [Fig. 3(a)], is observed, though the layering peak's position is  $\phi$  independent. A similarly fixed position but varying intensity is observed for the layering peak of the Hg-vapor interface upon variation of  $T$  [8].

$R/R_F$  is directly related to the laterally averaged surface-normal electron density profile  $\langle \rho_e(z) \rangle$  [18]. Since most of the electrons are localized in the ion cores,  $\langle \rho_e(z) \rangle$  is dominated by the ionic density profile  $\langle \rho(z) \rangle$ .  $\langle \rho_e(z) \rangle$  is extracted by fitting the measured  $R(q_z)$  by a model, employed successfully to describe the electron density profile of the Hg-vapor interface [7,8], as a semi-infinite distorted crystal lattice. The atomic Hg layers are equally spaced at distances  $d$ , i.e., centered at positions

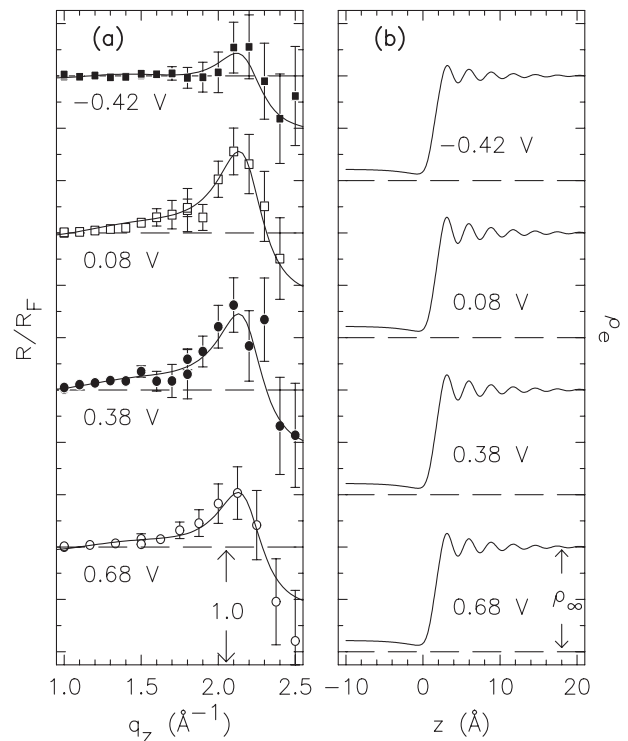


FIG. 2. (a) Measured (symbols) and model fitted (solid lines)  $R/R_F$  at the listed  $\phi$  values. (b) Interfacial electron density profiles calculated from the fits in (a).  $\rho_\infty = 3.25 \text{ e/\AA}^3$  is the bulk Hg electron density.

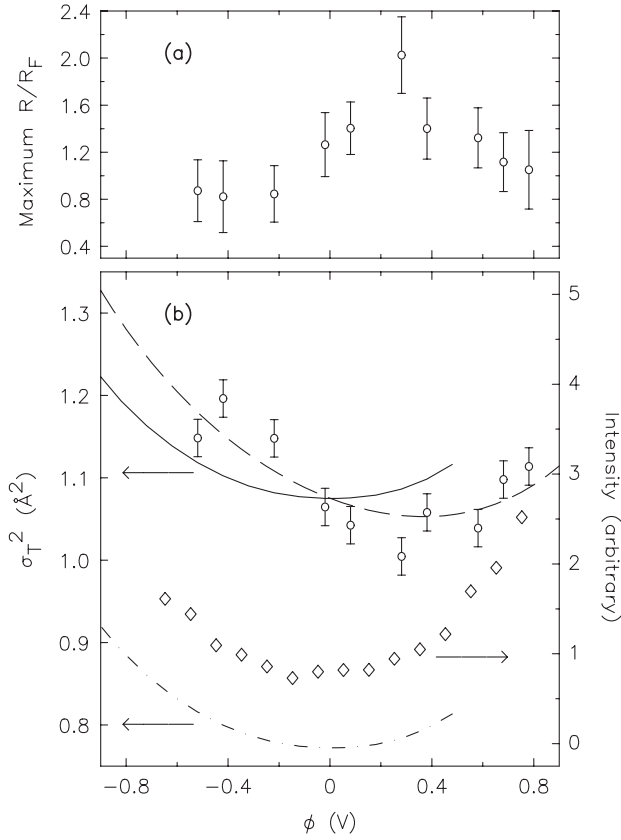


FIG. 3.  $\phi$  dependence of (a) the  $R/R_F$  layering peak's maximum, (b) the fit-refined  $\sigma_T^2$  ( $\circ$ ) with CW theory prediction  $\sigma_{CW}^2$  (dash-dot),  $\sigma_{CW}^2 + \Delta\sigma^2$  (line) and  $\sigma_{CW}^2 + \Delta\sigma^2 + a\phi$  (dashed). The diffuse scattering measured at  $q_z = 2.2 \text{ \AA}^{-1}$  and detector offset from the reflection plane by  $0.1^\circ$  ( $\diamond$ ) is also shown.

$p_n = nd$ . They are represented by fixed-area Gaussians of mean-squared surface-normal width  $\sigma_n$ , convoluted by the Fourier transformation of the normalized Hg structure factor. As  $n$  increases,  $\sigma_n$  increases and the initially well-defined individual layers broaden and merge into a constant-density bulk.  $\sigma_n = \sqrt{n\bar{\sigma}^2 + \sigma_T^2}$  has two contributions:  $\sigma_T$ , common to all layers and  $\bar{\sigma}$  which characterizes the broadening rate, and hence the decay rate of the layering with depth  $nd$ . The  $q_z$  position of the quasi-Bragg peak is determined by  $d$  as  $q_z = 2\pi/d$ , while  $\sigma_T$  and  $\bar{\sigma}$  determine its width. A low density adlayer residing above the first Hg layer is required to account for the shallow dip in  $R/R_F$  at  $q_z \approx 1 \text{ \AA}^{-1}$  [7,8]. The electrolyte's profile should in principle exhibit similar oscillations as that of Hg, as indeed found in molecular dynamics simulations of the liquid Hg-water interface [19]. However, this layering is much less pronounced and largely negligible if the capillary wave broadening is taken into account [20]. We therefore employ a simplified model where the electrolyte is described by an error function residing  $3 \text{ \AA}$  above the first atomic Hg layer, with a capillary wave width, which corresponds to the width of the Hg surface layer. Other

models with deviations in the density, spacing, and width of the topmost Hg layer were tested, but did not improve the agreement with experiment. Furthermore, within the experimental error the fit was found (within  $\pm 1 \text{ \AA}$ ) to be independent of the position of the error function describing the electrolyte, i.e., did not indicate  $\phi$ -dependent changes in the Hg-water spacing caused by the interface polarization.

Initial fits with all parameters free to vary showed that all  $R/R_F$  curves can be described by a  $\phi$ -independent  $d = 2.84 \pm 0.05 \text{ \AA}$ ,  $\bar{\sigma} = 0.46 \pm 0.05 \text{ \AA}$ , and a decay length of the layering amplitude into the bulk of  $6.0 \pm 0.3 \text{ \AA}$ . Allowing for resolution differences these values coincide, within their combined errors, with the  $T$ -independent  $d$  and  $\bar{\sigma}$  of the Hg-vapor interface [8], suggesting that these parameters are intrinsic properties of the liquid Hg. Interestingly, they differ by only 10% from those obtained by theoretical studies of the Hg-water interface [19], indicating the simple pairwise interatomic potentials employed in the simulations successfully describe the principal physical behavior. The parameters defining the adlayer are also  $\phi$ -independent. Only  $\sigma_T$  was found to vary with  $\phi$ .

In a second step of the fitting process all  $\phi$ -independent parameters were fixed at the obtained average values and only  $\sigma_T$  was varied. The resulting fits [Fig. 2(a), solid lines] provide a good description of the measured  $R/R_F$ . A small but distinct variation of the layering amplitudes with  $\phi$  is observed in the corresponding electron density profiles [Fig. 2(b)]. The resulting roughness values  $\sigma_T^2$ , shown in circles in Fig. 3(b), exhibit a clear parabolic  $\phi$  dependence. CW theory states that all liquid surfaces are decorated by thermally excited capillary waves of mean-amplitude  $\sigma_{CW}$  given by [21,22]:

$$\sigma_{CW}^2(\phi) = \frac{k_B T}{2\pi\gamma(\phi)} \ln\left(\frac{k_{\max}}{k_{\min}}\right) \quad (1)$$

with wave vector cutoffs determined by the atomic size and instrumental resolution, respectively,  $k_{\max} = 1.2 \text{ \AA}^{-1}$  [8] and  $k_{\min} = 7.8 \times 10^{-3} \text{ \AA}^{-1}$ , in our case.

$\sigma_{CW}^2(\phi)$  as calculated from this expression and published  $\gamma(\phi)$  values [14] [Fig. 3(b), dash-dot line], significantly underestimates the present experimental values (circles). A similar underestimation was found by DiMasi *et al.* [8] for the  $T$  dependence of  $\sigma_{CW}^2$  at the Hg-vapor interface. The latter carries no excess charge and hence corresponds to the electrochemical interface at the PZC. Indeed, the experimentally measured  $\sigma_T^2$  ( $T = 25^\circ \text{C}$ ) there coincides with  $\sigma_T^2$  ( $\phi = 0 \text{ V}$ ). Shifting up our calculated  $\sigma_{CW}^2(\phi)$  curve by the  $\Delta\sigma^2 \sim 0.3 \text{ \AA}^2$  offset found by DiMasi *et al.* at  $T = 25^\circ \text{C}$  [Fig. 3(b) solid line], brings it into better agreement with the general level of the measured  $\sigma_T^2(\phi)$ . However, the data are still shifted by  $\phi \approx +0.3 \text{ V}$  relative to the CW prediction, as manifest by the clear deviation of the minimum of the experimental

$\sigma_{\text{CW}}^2(\phi)$  dependence from the PZC. An almost perfect agreement with the experimental values is obtained upon the *ad hoc* addition of a linear term to the calculated  $\sigma_{\text{CW}}^2$ :  $\sigma_T^2(\phi) = \sigma_{\text{CW}}^2(\phi) + \Delta\sigma^2 + a\phi$ , where  $a = -0.1 \text{ \AA}^2/\text{V}$  (dashed line).

The CW-induced interfacial roughness can be probed directly by measuring the intensity it scatters out of the specular condition  $\beta = \alpha$  [18]. While a full quantitative study was not undertaken, the intensities measured at  $\Delta\beta = \beta - \alpha = 0.1^\circ$  [Fig. 3(b)] follow qualitatively the theoretically predicted parabolic  $\phi$  dependence, centered at  $\phi = 0 \text{ V}$ . This suggests that the linear offset term in  $\sigma_T^2(\phi)$  is not a CW-induced effect, but is rather due to  $\phi$ -induced changes in the intrinsic electron density profile at the Hg-electrolyte interface. These changes may originate in the polarization of the interface by the strong electric field of the electrochemical double layer. For a negative surface charge ( $\phi < 0 \text{ V}$ ) an increased spillover of electrons of the Hg metal into the solution is expected, which should broaden the profile at the interface. Vice versa, for a positive surface charge, the electron profile should be compressed. Using an interface between a jellium metal and an electrolyte of hard sphere ions and dipoles, polarization of the conduction electrons in the double layer field and their contribution to the double layer capacitance have been addressed by the Schmickler-Henderson theory [5]. Across the 1.3 V wide double layer potential range, the position of the electron density center of mass, shifts by  $\sim 1 \text{ \AA}$  [5]. Calculations of the corresponding change of the total electron density profile (with the ion core electron distribution assumed to be potential independent) show a broadening of  $0.17 \text{ \AA}$ . This is in the same order of magnitude as the additional slope  $a$  to  $\sigma_T^2$  obtained experimentally for the Hg-electrolyte interface, supporting the tentative assignment to a polarization effect. Additional contributions may come from polarization of the ion cores, which is neglected in the Schmickler-Henderson theory, and the rearrangement of species on the electrolyte side of the interface (e.g., water molecules).

In summary, we presented the first atomic-resolution XR study of the structure of a liquid-liquid interface, that of the Hg-electrolyte interface, a pivotal electrochemical system. Our results show that the depth-decaying surface-adjacent atomic layering observed at liquid-gas interfaces [7,8] persists at liquid-liquid interfaces with virtually the same structural properties. Varying the applied potential  $\phi$  revealed two intriguing anomalous effects: a significant increase in the surface roughness beyond that predicted by CW theory, and a  $\sim 0.3 \text{ V}$  shift in the vertex of the parabolic  $\phi$  dependence of the roughness. The origin of the former effect, identical to that observed for the Hg-vapor

interface [8] but for no other liquid metal studied to date, remains a mystery. The latter phenomenon we tentatively assign to interface polarization effects induced by the strong electric field of the double layer [5]. These results should provide a deeper insight into the atomic-scale structure of the liquid metal-electrolyte interface, and allow direct verification of modern double layer theories. They may be easily extended to related interfacial processes and effects, e.g., adsorption, alloying, and segregation phenomena, that take advantage of the unique properties of electrochemical interfaces, such as high reversibility, potential control, and the possibility for studies under reaction conditions. More generally, they open the way for future microscopic studies of liquid-liquid interfaces, allowing us to develop a comprehensive, atomic-scale picture of these complex systems.

We thank BMBF (project 05KS7FK3) and USA-Israel BSE, Jerusalem for funding. BNL and APS are supported by DOE contracts DE-AC02-76CH0016 and W-31-109-Eng-38, respectively.

---

\*murphy@physik.uni-kiel.de

- [1] G. Lippmann, Ann. Phys. (Leipzig) **225**, 546 (1873).
- [2] H. L. F. Helmholtz, Ann. Phys. (Leipzig) **243**, 337 (1879).
- [3] G. Gouy, J. Phys. Theor. Appl. **9**, 457 (1910).
- [4] D. L. Chapman, Philos. Mag. **25**, 6 (1913).
- [5] W. Schmickler and D. Henderson, Prog. Surf. Sci. **22**, 323 (1986).
- [6] S. A. Rice, Mol. Simul. **29**, 593 (2003).
- [7] O. M. Magnussen *et al.*, Phys. Rev. Lett. **74**, 4444 (1995).
- [8] E. DiMasi *et al.*, Phys. Rev. B **58**, R13419 (1998).
- [9] M. J. Regan *et al.*, Phys. Rev. Lett. **75**, 2498 (1995).
- [10] H. Tostmann *et al.*, Phys. Rev. B **59**, 783 (1999).
- [11] O. Shpyrko *et al.*, Phys. Rev. B **67**, 115405 (2003).
- [12] P. Pershan *et al.*, Phys. Rev. B **79**, 115417 (2009).
- [13] N. Lei, Z. Huang, and S. A. Rice, J. Chem. Phys. **104**, 4802 (1996).
- [14] N. H. Cuong *et al.*, J. Electroanal. Chem. **51**, 377 (1974).
- [15] G. M. Luo *et al.*, Science **311**, 216 (2006).
- [16] L. Bosio *et al.*, J. Electrochem. Soc. **139**, 2110 (1992).
- [17] D. C. Grahame, Chem. Rev. **41**, 441 (1947).
- [18] P. S. Pershan and J. Als-Nielsen, Phys. Rev. Lett. **52**, 759 (1984).
- [19] J. Böcker, Z. Gurskii, and K. Heinzinger, J. Phys. Chem. **100**, 14969 (1996).
- [20] E. Spohr, in *Advances in Electrochemical Science and Engineering*, edited by R. C. Alkire and D. M. Kolb (Wiley, Weinheim, 1999), Vol. 6, p. 1.
- [21] B. M. Ocko *et al.*, Phys. Rev. Lett. **72**, 242 (1994).
- [22] A. Braslau *et al.*, Phys. Rev. A **38**, 2457 (1988).